Journal of Aridland Agriculture 2023, 9: 1-8
doi: 10.25081/jaa.2023.v9.7464
https://updatepublishing.com/journal/index.php/jaa

Research Article

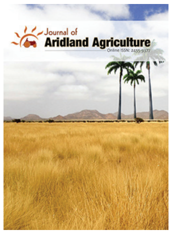

ISSN: 2455-9377

Monitoring of crop water consumption changing based on remotely sensed data and techniques in North Sinai, Egypt

M. A. El-Shirbeny[1,2]*, S. Orlandini[2,3]

[1]National Authority for Remote Sensing and Space Sciences (NARSS), Egypt, [2]Department of Agrifood Production and Environmental Sciences (DISPAA), University of Florence, Italy, [3]Climate and Sustainability Foundation (FCS), Italy

Received: September 06, 2022
Revised: January 21, 2023
Accepted: January 23, 2023
Published: February 10, 2023

***Corresponding Author:**
M. A. El-Shirbeny
E-mail: mshirbeny@yahoo.com

ABSTRACT

This paper aims to approximate and verify crop water use based on satellite results. Land Surface Temperature (*LST*) and Normalized Difference Vegetation Index (NDVI) were used as the critical parameters derived from *NOAA/AVHRR* and landsat8 satellite data. Reference evapotranspiration (*ETo*) was determined using FAO-Penman-Monteith (*FPM*) agrometeorological data as a standard process. Based on data from remote sensing, the *ETo* was calculated based on the Hargreaves (*Har*) process. *ETo-FPM* has been used to calibrate *ETo-Har* under the same conditions for five years (2002-2006). Landsat8 data was obtained on 25 June 2013 and 28 June 2014 and used to estimate the crop coefficient (*Kc*) based on satellite data (*Kc-Sat*). The *LST* was used to predict the maximum, minimum, and mean *Tair* (°C) levels in June 2013 and 2014. *ETo* was calculated using the expected maximum, minimum, and mean *Tair* according to the *Har* method and was used with *Kc-Sat* to estimate *ETc-Har*. *ETo-FPM* is used to measure *ETc-FPM* with *Kc-Sat*. *LST* and *NDVI* have been used to measure the Water Deficiency Index (*WDI*). *WDI* incorporated *ETc* to measure the actual evapotranspiration of the crop (*ETa*). *ETa-FPM* was used for the evaluation of *ETa-Har*. The relationship between *ETa-FPM* and *ETa-Har* was high, where R^2 was 0.99 in 2013 and 2014. *ETa* determined by Hargreaves based on remotely sensed data was overestimated at about 0.8 (mm/day) compared to the *FPM* process.

KEY WORDS: Hargreaves (*Har*), FAO-penman-monteith (*FPM*), Water deficit index (*WDI*), Actual evapotranspiration (ET_a), *NOAA/AVHRR*, and landsat8.

INTRODUCTION

North Sinai is a highly desirable area for agricultural production since most crops are grown with decent soil and a proper environment. In the study region, water shortage is a significant issue, and farmers depend on rainfall and minimal groundwater water.

To enhance irrigation water conservation, multiple models were used and built to measure ETo (El-Shirbeny *et al.*, 2011, Alblewi *et al.*, 2015; Zhao *et al.*, 2015; El-Shirbeny *et al.*, 2019). In both tropical and arid weather environments, the FPM model is the most precise approach (Yin *et al.*, 2008; El-Shirbeny & Abdellatif, 2017; El-Shirbeny *et al.*, 2021a; Gamal *et al.*, 2022; Afify *et al.*, 2023).

ETc is evaluated based on a so-called two-step method. ETo is first calculated, and all other crops and environmental factors are then taken into consideration using the semi-empirical coefficient (kc) (Allen *et al.*, 1998; Magliulo *et al.*, 2003; Silva *et al.*, 2012; Kamble *et al.*, 2013; El-Shirbeny *et al.*, 2015, 2021b, 2022; Gamal *et al.*, 2022). Potential modeling of Kc as a feature of the vegetation index was suggested by comparisons between the Kc curve and the satellite-derived vegetation index (Kamble *et al.*, 2013). The possibility of measuring Kc directly from satellite data was then examined (Magliulo *et al.*, 2003; El-Shirbeny *et al.*, 2014b, 2014c; El-Shirbeny & Saleh, 2021).

Remotely sensed data and strategies for irrigation water management have been studied and used effectively in recent years to estimate ETa and ETc (Rwasoka *et al.*, 2011; Merlin *et al.*, 2014; El-Shirbeny *et al.*, 2014a, 2014b, 2014d, 2015; Hu *et al.*, 2015; Tadesse *et al.*, 2015). Satellite data is used to track the tension of crop water for the specific management of agriculture and monitor crop behaviours (Ghulam *et al.*, 2008; Aboelghar *et al.*, 2010, 2011; Tolba, *et al.*, 2020; Ali *et al.*, 2021; Mohamed *et al.*, 2021).

The water deficit index (WDI) is a function of the ratio of ETa to ETc (Hiler & Clark, 1971). Various satellite data, such as Landsat, NOAA/AVHRR, and MODIS, were used to measure WDI. To approximate WDI at two sites with different climatic influences on ETa in Andalusia-Spain, a MODIS index dependent on the spatial relationship between LST and NDVI was evaluated by (Garcia *et al.*, 2014). The primary purpose of this paper is to use data and techniques that are remotely sensed to approximate the actual evapotranspiration in North Sinai.

MATERIALS AND METHODS

Study area

The study area is located in the northeast of Egypt (Rafah to El-Arish), and the total area is 116747 Ha (1167.47Km^2), as shown in Figure 1.

During the winter, irrigation in North Sinai relies on precipitation, but during the summer, it relies on underground water or water collected during the rainy season. A typical irrigation system in the study region is drip irrigation.

Low rainfall, high temperatures, mild wind, and high relative humidity define the dominant macro-climate parameters. The data were obtained from the meteorological station in El-Arish. At latitude 31.27 N, longitude 33.75 E, and elevation 15 m (a.s.l.), it was installed at 2 m above ground level. From 1985 to date, the values of Tair, relative humidity, wind speed, and rainfall were reported.

Satellite data

Satellite data from the NASA database can be viewed on the internet. The NASA database was used to cover the study area; NOAA/AVHRR (advanced very high resolution radiometric) was used for the measurement of Kc and ETo from 1 June to 30 June 2006 and 2007 with 1100 m ground resolution and Landsat-8 data acquired on 25 June 2013 and 28 June 2014.

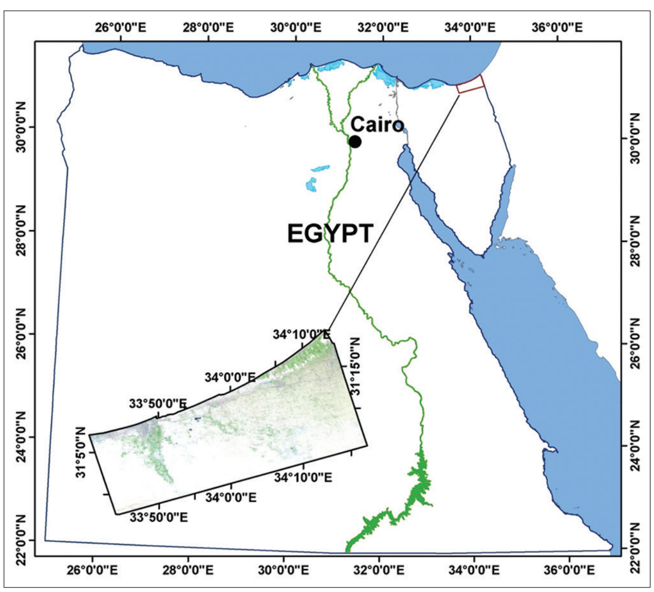

Figure 1: Shows the study area location

Extracting of *LST* and *NDVI*

NOAA data was analyzed by pursuing this procedure:- a) collection of clear-sky satellite overpasses; b) georeferencing data; c) 10-day average generation of NDVI data; d) 9-pixel computation implies LST over ground-based station location. The retrieved emissivity determined by Valor and Caselles (1996) (eq. 2, 3, and 4) algorithm is used by Sobrino *et al.* (1993) (equation 1), using the NDVI as a representative of the emissive characteristics. The emissivity vector was obtained as follows:-

$$LST = T_4 + [0.53 + 0.62(T_4 - T_5)]\,(T_4 - T_5) + 64(1 - \varepsilon) \qquad (1)$$

Where: T4 and T5 are brightness temperatures for channels 4 and 5 of *AVHRR*, and ε is mean emissivity for channels 4 and 5, $(\varepsilon_4 + \varepsilon_5)/2$.

$$\varepsilon = 0.985Pv + 0.96(1\text{-}Pv) + 0.06Pv\,(1\text{-}Pv) \qquad (2)$$

Thus:

$$Pv = \frac{(1 - i/ig)}{(1 - i/ig) - k(1 - i/iv)} \qquad (3)$$

and k is:

$$k = \frac{\rho 2v - \rho 1v}{\rho 2g - \rho 1g} \qquad (4)$$

Where: *i*, *ig*, and *iv* are *NDVI*, *NDVI* bare soil, *NDVI* vegetated surface, ρ_1 and ρ_2 are channels 1 and 2 reflectance's of *AVHRR*, and *v* and *g* are indexes for vegetation and bare soil. The monthly mean *NDVI* values for bare soil and vegetated areas are presented in Table 1.

The collected digital numbers (DN) for landsat8 data have been translated to radiance units (Rad) using calibration coefficients unique to each section.

Band 10 is used to extract *LST* as follows:-

$$\text{Radiance} = 0.0003342 * DN + 0.10000 \qquad (5)$$

Surface emissivity (*Eo*) was estimated from the *NDVI* using the empirical equation developed from raw data on *NDVI* and thermal emissivity (Valor & Caselles, 1996).

Table 1: Illustrates *NDVI* values for bare soil and vegetated area from *NOAA/AVHRR*

Month	*NDVI*	
	Bare soil	Vegetation
June 2006	0.03	0.12
June 2007	0.04	0.12

$$Eo = 0.9932 + 0.0194 \ln NDVI \quad 6)$$

The radiant temperature (*To*) can be calculated from band 10 radiance (*Rad10*) using calibration constants K_1=774.89 and K_2=1321.08.

$$To = K_2/\ln((K_1/Rad10) + 1) \quad (7)$$

The radiant satellite temperature of the viewed Earth-atmosphere system is the corresponding temperature (Kelvin), which is correlated with, but not the same as, the surface (kinetic) temperature. To achieve a precise estimation of surface temperature from satellite thermal records, the atmospheric effects and surface thermal emissivity have to be considered (Norman *et al.*, 1995). From the top of the ambient radiant temperature (To) and measured surface emissivity (Eo), the LST is determined as:

$$LST = To/Eo \quad (8)$$

Reference evapotranspiration (ET_o) estimation

Using the FPM method equation (9) prepared by Allen *et al.* (1998), ETo was computed from meteorological evidence.

$$ETo = \frac{0.408\Delta(R_n - G) + \gamma \frac{900}{T+273} u_2(e_s - e_a)}{\Delta + \gamma(1 + 0.34u_2)} \quad (9)$$

Where; *ETo*, reference evapotranspiration [mm day-1], *Rn*, net radiation at the crop surface [MJ m-2 day-1], *G*, soil heat flux density [MJ m-2 day-1], *T*, mean daily air temperature at 2 m height [°C], u_2, wind speed at 2 m height [m s-1], *es*, saturation vapor pressure [kPa], *ea*, actual vapor pressure [kPa], *es - ea*, saturation vapor pressure deficit [kPa], Δ, slope vapor pressure curve [kPa °C-1], γ, psychrometric constant [kPa °C-1].

The Hargreaves method was used to approximate ETo from the expected Tair hourly equation (10) under the same conditions after calibration with FPM (El-Shirbeny *et al.*, 2016). In the case of low data availability, such as in northern Sinai, the FAO organization suggested this process. Minimum details, maximum, minimum, average air temperature, number of days, and latitude of the research region are used in this process. From estimations based on Landsat8 satellite results, the meteorological parameters used in this equation were obtained.

$$ETo = 0.0023(T_{mean} + 17.8)(T_{max} - T_{min})^{0.5} * R_a \quad (10)$$

Where; T_{mean} is the average daily temperature (°C), T_{max} is the maximum temperature (°C), T_{min} is the minimum temperature (°C), and R_a is the extraterrestrial radiation. For each day of the year and different latitudes, it could be estimated from the solar constant.

Ra is the extra-terrestrial light, from the solar constant, the solar declination, and the period of the year with each day of the year and various latitudes may be calculated by:—

$$R_a - \frac{24(60)}{\pi} G_{so} d_r [\omega_s \sin(\phi)\sin(\sigma) + \cos(\phi)\cos(\sigma)\sin(\omega_s)] \quad (11)$$

Where; R_a is extraterrestrial radiation [MJ m-2 day-1], G_{so} is solar constant (0.0820 MJ m-2 min-1), d_r is inverse relative distance Earth-Sun, ω_s is sunset hour angle [rad], *j* is latitude [rad], *d* is solar declination [rad]. The corresponding equivalent evaporation in (mm day-1) is obtained by multiplying R_a by 0.408. The latitude (*j*) expressed in radians is positive for the northern hemisphere and negative for the southern hemisphere.

The inverse relative distance Earth-Sun (dr) and the solar declination (δ) are given by:

$$dr = 1 + 0.033 * \cos(2 * Л * J/365) \quad (12)$$

$$\delta = o.409 * \sin((2 * Л * J/365) - 139) \quad (13)$$

Where: *J* is the number of the day in the year between 1 (1 January) and 365 or 366 (31 December), and the sunset hour angle (ω_s) is given by:

$$\omega s = \arccos[-\tan(j)\tan(d)] \quad (14)$$

As the arccos function is not available in all computer languages, the sunset hour angle can also be computed using the arctan function:

$$\omega_s = (Л/2) - \arctan[-\tan(\phi) * \tan(\delta)/X0.5] \quad (15)$$

Where:-

$$X = 1 - [\tan(j)]^2 [\tan(d)]^2 \text{ and } X = 0.00001 \text{ if } X £ 0 \quad (16)$$

Crop coefficient (K_c) estimation

K_c is a dimensionless number (usually between 0.1 and 1.2) used to calculate (ET_c). The relation between K_c and *NDVI* is represented by equation (17), used by El-Shirbeny *et al.* (2014b) and calibrated for wheat by El-Shirbeny *et al.* (2014c).

$$Kc = \frac{1.2}{NDVI_{dv}}(NDVI - NDVI_{mv}) \quad (17)$$

Where; 1.2 is the maximum K_c under Egyptian conditions, $NDVI_{dv}$ is the difference between the minimum and maximum *NDVI* value for vegetation, and $NDVI_{mv}$ is the minimum *NDVI* value for vegetation.

Water deficit Index (*WDI*) and ET_a estimation

Moran *et al.* (1994) developed the *WDI* method to measure the amount of ET_a occurring to the ET_c (equation 18).

$$WDI = 1 - \frac{\text{ETa}}{\text{ETc}} \quad (18)$$

WDI uses both *LST* subtracting T_{air} and a vegetation index to estimate the relative water status of a field (equation 19).

$$WDI = \frac{\Delta T - \Delta Tm}{\Delta Tx - \Delta Tm} \tag{19}$$

Where: ΔT is the difference between measured surface and air temperature, ΔTm is the difference between minimum surface and air temperature, and ΔTx is the difference between maximum surface and air temperature.

RESULTS AND DISCUSSION

Minimum, Maximum, and Mean T_{air} Prediction

Particularly with the surface water status, the roughness duration, and the wind speed, the difference between Tair and LST differs. The relation between Tair and LST in the thermodynamics of the biosphere is always quite elusive due to certain physical conditions. To forecast Tair from LST, this relationship was used. At night, LST was lower than Tair, but it was the reverse on the day, owing to the higher surface energy released and wind speed and air humidity influencing Tair. Due to clouds, the amount of data during the night was smaller than during the day. Figure 2a indicates the relationship in the El-Arish area between Tair (°C) and LST (°C) derived from NOAA/AVHRR 17 and 18. Mean hourly Tair (Figure 2b) was used to predict min, max, and mean Tair.

Hargreaves method compared with *FPM*

ETo was estimated under the same conditions for five years (2002-2006) using agro-meteorological data according to Hargreaves and FPM methods. The majority of ETo values measured using Hargreaves were relatively high; 15 mm/day was achieved. Because the Mediterranean Sea's closest research location and several variables such as wind speed and relative humidity will influence it, and the Hargreaves approach relies on a few parameters, it must be adjusted with a standard method such as FPM or Lysimeter.

Allen *et al.* (1989) analyzed common Penman equation forms and general ETo estimation relationships. They made a correlation between the penman equation corrected for FAO-24 and Lysimeter. They also formed a partnership between Kimberly-Penman and Penman-Monteith v. Lysimeter in 1982.

Besides the Penman-Monteith, all methods used in the regular study were modified using the 1.15 multiplier for the Lysimeter vegetation sort. Compatibility with paper guidelines (Allen *et al.*, 1989) and FAO56; Evapotranspiration measured under the same conditions and period using the Hargreaves system was adjusted using the FPM process. Figure 3a shows the relationship between the ETo determined by the Hargreaves method and the meteorological data-based FPM process, and Figure 3b displays the ETo-Har compared with FPM after calibration. A strong connexion was given where R2 = 0.78. On the other hand, the relationship between ETa determined by Hargreaves and FPM based on remotely sensed data, as seen in Figure 4, and R2 was strong at 0.99 on 25 June 2013 and 28 June 2014, respectively.

ET_c estimation

For real-time irrig=ation calculation, exact regular ETo monitoring is required. Luo *et al.* (2014) suggested a system

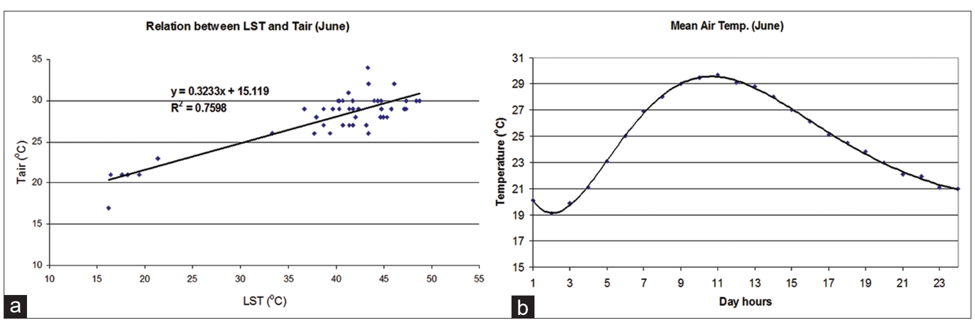

Figure 2: (a) Shows the relation between T_{air}(oC) and *LST* (oC) In the El-Arish region, and (b) Shows the average hourly T_{air} for June month

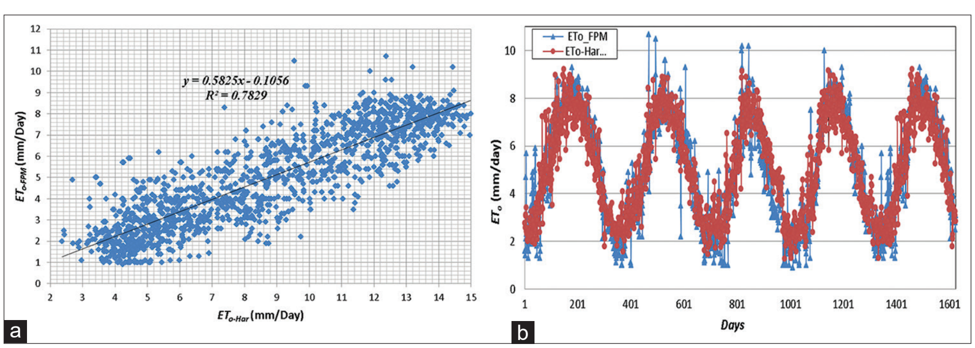

Figure 3: (a) shows the relation between ET_o by Hargreaves and *FPM* and (b) shows the validation of $ET_{o\text{-}Har}$ compared with *FPM*

to uses the locally tuned Hargreaves-Samani model and temperature predictions to predict ETo in the short term. Bois *et al.* (2008) focused on satellite data and ground stations, using FPM, Hargreaves, and Radiation methods to measure reference evapotranspiration. After calibration with FPM, ETo was extracted from Landsat8 data as per Hargreaves. Figure 5 displays the Hargreaves-estimated ETo after calibration. It ranged from 5 to 10.5 (mm/day) on 25 June 2013 and from 7 to 10.5 (mm/day) on 28 June 2014.

Kc depends on the height of the canopy, crop growth, design, and cover stage (Allen *et al.*, 1998). There is an excellent link between the interaction between Kc and NDVI. NDVI was determined from the Red and NIR bands of Landsat8 data acquired on 25 June 2013 and 28 June 2014, respectively. Values in the range of -1.0 to 1.0 are created by the NDVI equation, where vegetated areas usually have values greater than 0.2, and lower values represent non-vegetated surface characteristics, such as water, ice, snow, or clouds. Depending on crop age, planting density, and chlorophyll operation, NDVI varies. It looks like the Kc curve from planting to senescence, which reflects the life cycle. Figure 6 shows the variance of Kc values according to Landsat8 data in the study region. Kc ranged from 0 to 1.2 in the sample region.

ET_o and K_c were used to estimate ET_c. $ET_{c\text{-}FPM}$ values varied from 0 to 6 and 7.5 (*mm/day*) on the 25th of June 2013 and 28th of June 2014, respectively. $ET_{c\text{-}Har}$ values varied from 0 to 7 and 8.5 (*mm/day*) on the 25th of June 2013 and 28th of June 2014, respectively. Figure 7 shows ET_c distribution in the study area.

WDI and ET_a estimation

Stomata are closed while plants are underwater tension, which causes transpiration to stop, increasing leaf temperature (Jackson *et al.*, 1981). The response of crop yield to water

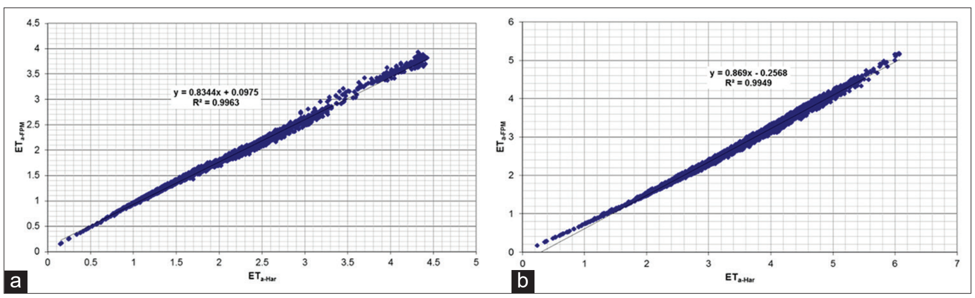

Figure 4: (a) shows the relation between ET_a estimated by Hargreaves and *FPM* on the 25th of June 2013 and (b) shows the relation between ET_a estimated by Hargreaves and *FPM* on 28th of June 2014

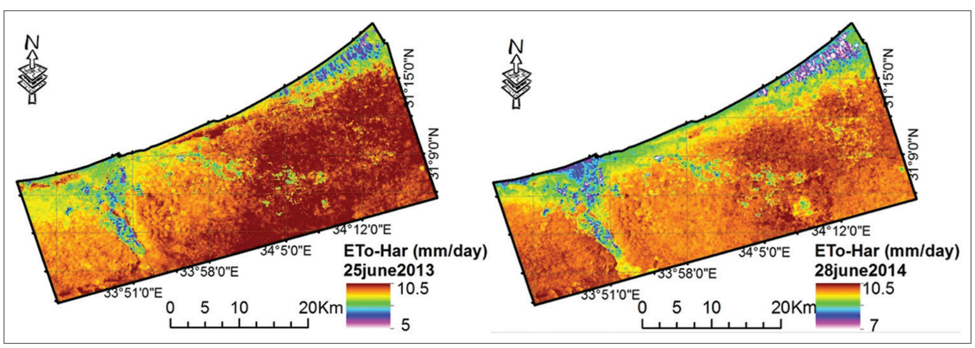

Figure 5: ET_o estimated by Hargreaves after calibration with *FPM*

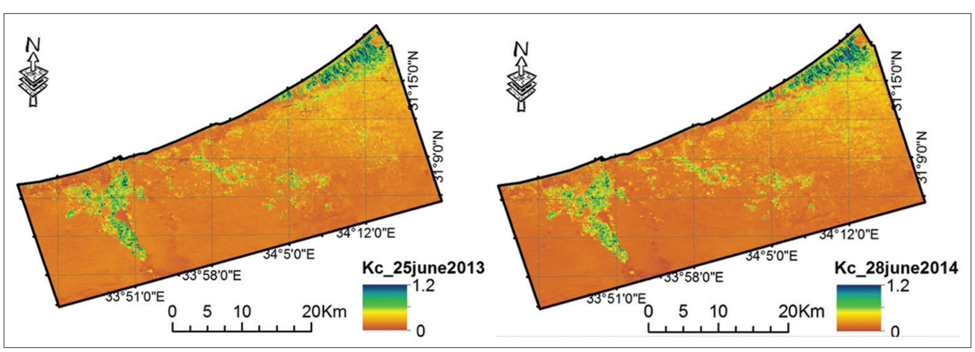

Figure 6: K_c extracted from Landsat8 according to equation no. (18)

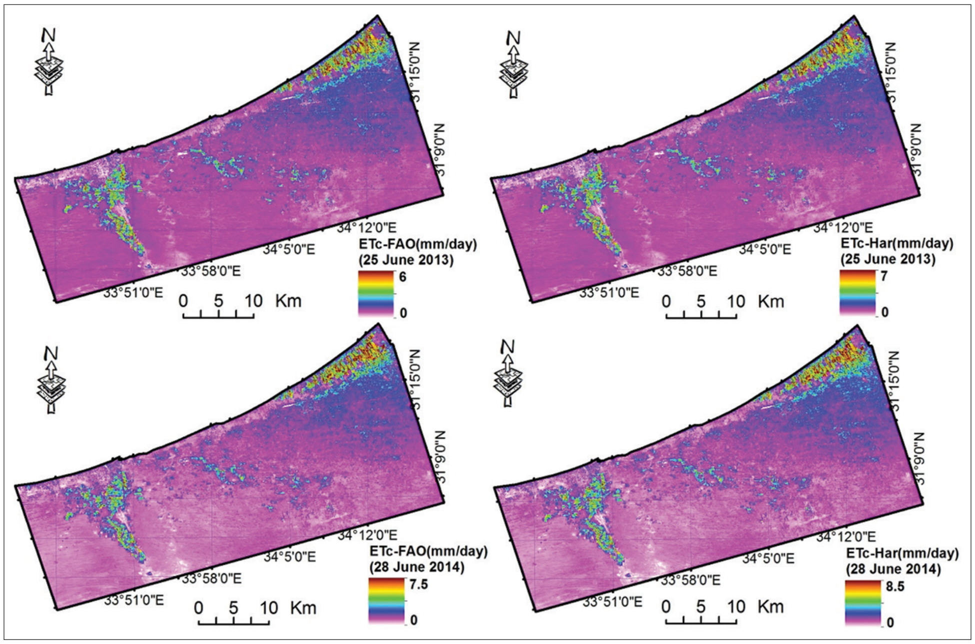

Figure 7: ET_c distribution in the study area

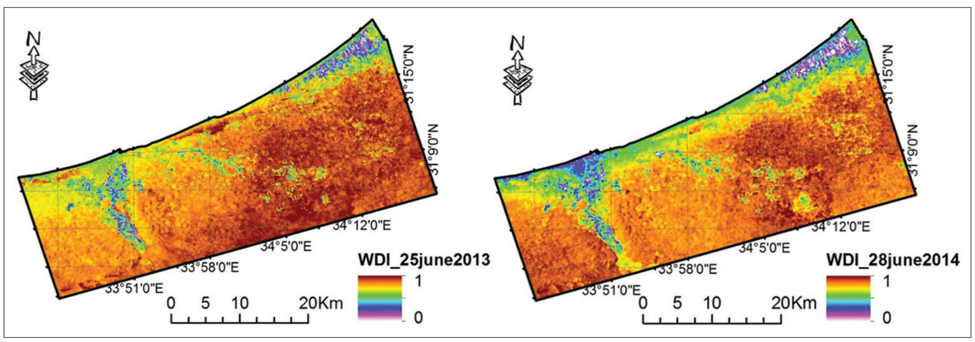

Figure 8: *WDI* distribution in the study area

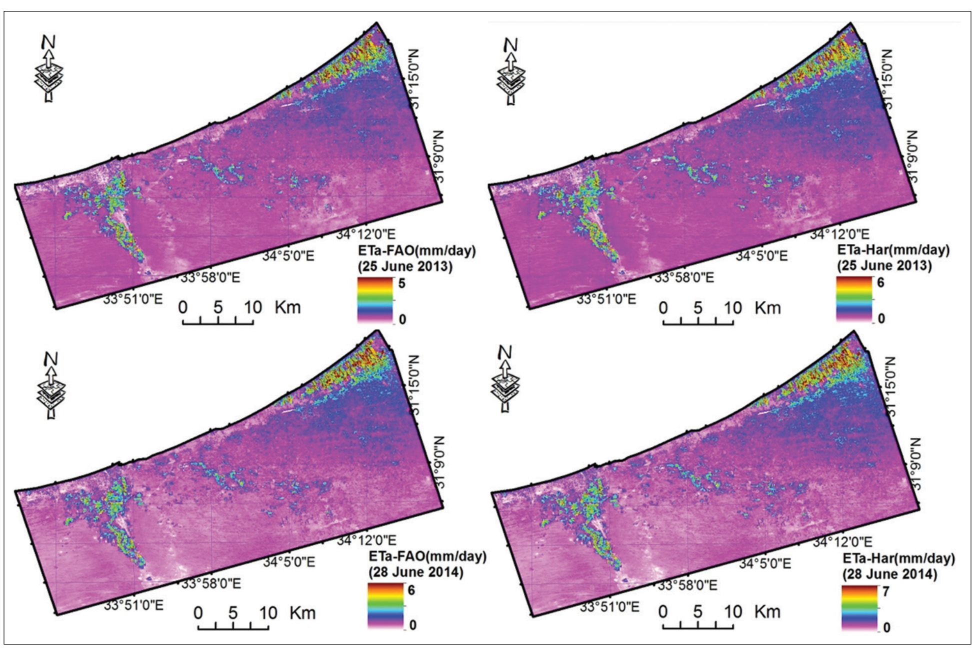

Figure 9: ET_a distribution in the study area

stress differs with the form of the crop and differs with the atmosphere. For a single crop in various climates and soils to be used in yield estimation and irrigation scheduling, the values of WDI can be calculated (Erdem *et al.*, 2006). The canopy would not fully cover the surface of the soil during the early season of annual crops and specific cultivation systems, and the dry soil is also much colder than Tair. Moran *et al.* (1994) created the WDI to solve this issue since the context of the canopy used in LST will contribute to false indications of water tension. WDI influenced changes in LST and Tair. A WDI value of 0 reveals no water stress, and a value of 1 suggests maximum water stress (Figure 8).

In arid and semi-arid ecosystems, based on water regimes, ET varies across a broad spectrum. Moreover, all the other mutually related factors are automatically influenced by the variation of one temperature parameter. This reality makes it hard to determine the ETa properly (Rana & Katerji, 2000). Er-Raki *et al.* (2007) evaluated the efficacy of three approaches focused on the FAO-56 Kc methodology to predict ETa for winter wheat in Morocco's semi-arid conditions under various irrigation treatments. ETa has been calculated in line with Equation (18). It was influenced by the WDI and ETc shifts. The ETa-FPM values on 25 June 2013 and 28 June 2014 ranged from 0 to 5 and 6 (mm/day), respectively, while the ETa-Har values on 25 June 2013 and 28 June 2014 ranged from 0 to 6 and 7 (mm/day), respectively. An increase in ETa according to land cover type, crop level, weather conditions, and water stress conditions was observed, as shown in Figure 9.

CONCLUSION

In arid and semi-arid areas, *ETa* is the most essential desired parameter for assessing crop water consumption. *ETa* can be measured across various models that differ in complexity, but the precision of the *ETa* assessment is proportional to the degree of validation and calibration. Restricting ground data is a real issue in Egypt and developing countries. Alternatively, satellite data are used after validation or calibration, especially in the agricultural field. Hargreaves after calibration with *FPM* is an appropriate method for calculating *ETo* in low-accessible data counties. *ETa* determined by Hargreaves based on remotely sensed data was overestimated by approximately 0.8 (*mm/day*) associated with the *FPM* process. Scheduling irrigation policies with remotely sensed methods would be more straightforward. It could be a valuable and low-cost tool for evaluating the supply of crop water and enhancing water management by regulating water use and increasing agricultural sustainability.

ACKNOWLEDGMENT

I'd like to thank NASA for making the data available. The Egyptian Cultural Affairs and Mission Sector funded this study.

REFERENCES

Aboelghar, M., Arafat, S., Abo Yousef, M., El-Shirbeny, M., Naeem, S., Massoud, A., & Saleh, N. (2011). Using SPOT data and leaf area index for rice yield estimation in Egyptian Nile delta. *The Egyptian Journal of Remote Sensing and Space Science, 14*(2), 81-89. https://doi.org/10.1016/j.ejrs.2011.09.002

Aboelghar, M., Arafat, S., Saleh A., Naeem, S., El-Shirbeny, M., & Belal, A. (2010). Retrieving leaf area index from SPOT4 satellite data. *The Egyptian Journal of Remote Sensing and Space Science, 13*(2), 121-127. https://doi.org/10.1016/j.ejrs.2010.06.001

Afify, N. M., El-Shirbeny, M. A., El-Wesemy, A. F., & Nabil, M. (2023). Analyzing satellite data time-series for agricultural expansion and its water consumption in arid region: a case study of the Farafra oasis in Egypt's Western Desert. Euro-Mediterranean Journal for Environmental Integration, 2023. https://doi.org/10.1007/s41207-022-00340-4.

Alblewi, B., Gharabaghi, B., Alazba, A., & Mahboubi, A. (2015). Evapotranspiration models assessment under hyper-arid environment. *Arabian Journal of Geoscience, 8*, 9905-9912. https://doi.org/10.1007/s12517-015-1867-7

Ali, A. M., Savin, I., Poddubskiy, A., Abouelghar, M., Saleh, N., Abutaleb, K., El-Shirbeny, M., & Dokukin, P. (2021). Integrated method for rice cultivation monitoring using Sentinel-2 data and Leaf Area Index. *The Egyptian Journal of Remote Sensing and Space Science, 24*(3), 431-441. https://doi.org/10.1016/j.ejrs.2020.06.007

Allen, R. G., Jenesen, M. E., Wright, J. M., & Burman, R. D. (1989). Operational estimates of reference evapotranspiration. *Agronomy Journal, 81*(4), 650-662. https://doi.org/10.2134/agronj1989.00021962008100040019x

Allen, R. G., Perrier, L. S., Raes, D., & Smith, M. (1998). Crop evapotranspiration: Guidelines for computing crop water requirements. Irrigation and drainage paper No. 56, FAO, Rome, Italy. Retrieved from https://www.fao.org/3/x0490e/x0490e00.htm

Bois, B., Pieri, P., Van Leeuwen C., Wald, L., Huard, F., Gaudillere, J. P., & Saur, E. (2008). Using remotely sensed solar radiation data for reference evapotranspiration estimation at a daily time step. *Agricultural and Forest Meteorology, 148*(4), 619-630. https://doi.org/10.1016/j.agrformet.2007.11.005

El-Shirbeny, M. A., & Abdellatif, B. (2017). Reference Evapotranspiration Borders Maps of Egypt Based on Kriging Spatial Statistics Method. *International Journal of GEOMATE, 13*(37), 1-8. https://doi.org/10.21660/2017.37.63048

El-Shirbeny, M. A., & Saleh, S. M. (2021). Actual evapotranspiration evaluation based on multi-sensed data. *Journal of Aridland Agriculture, 7*, 95-102. https://doi.org/10.25081/jaa.2021.v7.7087

El-Shirbeny, M. A., Abdellatif, B., Ali A. M., & Saleh N. H. (2016). Evaluation of Hargreaves based on remote sensing method to estimate potential crop evapotranspiration. *International Journal of GEOMATE, 11*(23), 2143-2149.

El-Shirbeny, M. A., Aboelghar, M. A., Arafat, S. M., & El-Gindy, A.-G. M. (2011, October 7). Mutual influence between climate and vegetation cover through satellite data in Egypt. Proceeding of the SPIE 8174, Remote Sensing for Agriculture, Ecosystems, and Hydrology XIII. https://doi.org/10.1117/12.897920

El-Shirbeny, M. A., Aboelghar, M. A., Arafat, S. M., & El-Gindy, A.-G. M. (2014a). Assessment of the mutual impact between climate and vegetation cover using NOAA-AVHRR and Landsat data in Egypt. *Arabian Journal of Geoscience, 7*(4), 1287-1296. https://doi.org/10.1007/s12517-012-0791-3

El-Shirbeny, M. A., Ali, A. M., & Saleh, N. H. (2014b). Crop Water Requirements in Egypt Using Remote Sensing Techniques. *Journal of Agricultural Chemistry and Environment, 3*(2B), 57-65. https://doi.org/10.4236/jacen.2014.32B010

El-Shirbeny, M. A., Ali, A. M., Badra, M. A., & Bauomy, E. M. (2014c). Assessment of Wheat Crop Coefficient Using Remote Sensing Techniques. *World Research Journal of Agricultural Sciences, 1*(2), 12-16.

El-Shirbeny, M. A., Ali, A. M., Khdery, G. A., Saleh, N. H., Afify, N. M., Badr, M. A., & Bauomy, E. M. (2021a). Monitoring agricultural water in the desert environment of New Valley Governorate for sustainable agricultural development: a case study of Kharga. *Euro-Mediterranean Journal for Environmental Integration, 6*(2), 1-15. https://doi.org/10.1007/s41207-021-00256-5

El-Shirbeny, M. A., Ali, A. M., Savin, I., Poddubskiy, A., & Dokukin, P. (2021b). Agricultural Water Monitoring for Water Management Under Pivot Irrigation System Using Spatial Techniques. *Earth Systems and Environment, 5*(2), 341-351. https://doi.org/10.1007/s41748-020-00164-8

El-Shirbeny, M. A., Alsersy, M. A. M., Saleh, N. H., & Abu-Taleb, K. A. (2015).

Changes in irrigation water consumption in the Nile Delta of Egypt assessed by remote sensing. *Arabian Journal of Geoscience, 8*, 10509-10519. https://doi.org/10.1007/s12517-015-2005-2
El-Shirbeny, M. A., Biradar, C., Amer, K., & Paul, S. (2022). Evapotranspiration and Vegetation Cover Classifications Maps Based on Cloud Computing at the Arab Countries Scale. *Earth Systems and Environment, 6*, 837-849. https://doi.org/10.1007/s41748-022-00320-2
El-Shirbeny, M. A., Mohamed, E. S., & Negm, A. (2019). Estimation of Crops Water Consumptions Using Remote Sensing with Case Studies from Egypt. In A. m. Negm (Ed.), *Conventional Water Resources and Agriculture in Egypt* (Vol. 74, pp. 161-186) Cham, Switzerland: Springer. https://doi.org/10.1007/698_2018_305
El-Shirbeny, M. A., Saleh, N. H., & Ali, A. M. (2014d). Estimation of Potential Crop Evapotranspiration Using Remote Sensing Techniques. Proceedings of the 10th International Conference of AARSE (pp. 460-468).
Erdem, Y., Sehirali, S., Erdem, T., & Kenar, D. (2006). Determination of Crop Water Stress Index for Irrigation Scheduling of Bean (Phaseolus vulgaris L.). *Turkish Journal of Agriculture and Forestry, 30*(3), 195-202.
Er-Raki, S., Chehbouni, A., Guemouria, N., Duchemin, B., Ezzahar, J., & Hadria, R. (2007). Combining FAO-56 model and groundbased remote sensing to estimate water consumption of wheat crops in semi-arid regions. *Agricultural Water Management, 87*(1), 41-54. https://doi.org/10.1016/j.agwat.2006.02.004
Gamal, R., El-Shirbeny, M., Abou-Hadid, A., Swelam, A., El-Gindy, A.-G., Arafa, Y., & Nangia, V. (2022). Identification and Quantification of Actual Evapotranspiration Using Integrated Satellite Data for Sustainable Water Management in Dry Areas. *Agronomy, 12*(9), 2143. https://doi.org/10.3390/agronomy12092143
Garcia, M., Fernández, N., Villagarcía, L., Domingo, F., Puigdefábregas, J., & Sandholt, I. (2014). Accuracy of the Temperature–Vegetation Dryness Index using MODIS under water-limited vs. energy-limited evapotranspiration conditions. *Remote Sensing of Environment, 149*, 100-117. https://doi.org/10.1016/j.rse.2014.04.002
Hiler, E. A., & Clark, R. N. (1971). Stress day index to characterize effects of water stress on crop yields. *Transactions of American Society of Agricultural and Biological Engineers, 14*(4), 757-761. https://doi.org/10.13031/2013.38384
Hu, G., Jia, L., & Menenti, M. (2015). Comparison of MOD16 and LSA-SAF MSG evapotranspiration products over Europe for 2011. *Remote Sensing of Environment, 156*, 510-526. https://doi.org/10.1016/j.rse.2014.10.017
Jackson, R. D., Idso, S. B., Reginato, R. J., & Pinter, J. R. (1981). Canopy temperature as a crop water stress indicator. *Water Resources Research, 17*(4), 1133-1138. https://doi.org/10.1029/WR017i004p01133
Kamble, B., Kilic, A., & Hubbard, K. (2013). Estimating Crop Coefficients Using Remote Sensing-Based Vegetation Index. *Remote Sensing, 5*(4), 1588-1602. https://doi.org/10.3390/rs5041588
Luo, Y., Chang, X., Peng, S., Khan, S., Wang, W., Zheng, Q., & Cai, X. (2014). Short-term forecasting of daily reference evapotranspiration using the Hargreaves–Samani model and temperature forecasts. *Agricultural Water Management, 136*, 42-51. https://doi.org/10.1016/j.agwat.2014.01.006
Magliulo, V., d'Andria, R., & Rana, G., (2003). Use of the modified atmometer to estimate reference evapotranspiration in Mediterranean environments. *Agricultural Water Management, 63*(1), 1-14. https://doi.org/10.1016/S0378-3774(03)00098-2
Merlin, O., Chirouze, J., Olioso, A., Jarlan, L., Chehbouni, G., & Boulet, G. (2014). An image-based four-source surface energy balance model to estimate crop evapotranspiration from solar reflectance/thermal emission data (SEB-4S). *Agricultural and Forest Meteorology, 184*, 188-203. https://doi.org/10.1016/j.agrformet.2013.10.002
Mohamed, E. S., Belal, A. A., Abd-Elmabod, S. K., El-Shirbeny, M. A., Gad A., & Zahran, M. B. (2021). Smart farming for improving agricultural management. *The Egyptian Journal of Remote Sensing and Space Science, 24*(3), 971-981. https://doi.org/10.1016/j.ejrs.2021.08.007
Moran, M. S., Clarke, T. R., Inoue, Y., & Vidal, A. (1994). Estimating crop water deficit using the relation between surface air temperature and spectral vegetation index. *Remote Sensing of Environment, 49*(3), 246-263. https://doi.org/10.1016/0034-4257(94)90020-5
Norman, J. M., Divakarla, M., & Goel, N. S. (1995). Algorithms for extracting information from remote thermal-IR observations of the Earth's surface. *Remote Sensing of Environment, 51*(1), 157-168. https://doi.org/10.1016/0034-4257(94)00072-U
Rana, G., & Katerji, N. (2000). Measurement and estimation of actual evapotranspiration in the field under Mediterranean climate: a review. *European Journal of Agronomy, 13*(2-3), 125-153. https://doi.org/10.1016/S1161-0301(00)00070-8
Rwasoka, D. T., Gumindoga, W., & Gwenzi, J. (2011). Estimation of actual evapotranspiration using the Surface Energy Balance System (SEBS) algorithm in the Upper Manyame catchment in Zimbabwe. *Physics and Chemistry of the Earth, 36*(14-15), 736-746. https://doi.org/10.1016/j.pce.2011.07.035
Silva, V. de P. R. da, Borges, C. J. R., Farias, C. H. A., Singh, V. P., Albuquerque, W. G., & Silva, B. B. da. (2012). Water requirements and single and dual crop coefficients of sugarcane grown in a tropical region, Brazil. *Agricultural Sciences, 3*(2), 274-286. https://doi.org/10.4236/as.2012.32032
Sobrino, J. A., Caselles, V., & Coll, C. (1993). Theoretical split-window algorithms for determining the actual surface temperature. *Il Nuovo Cimento C, 16*, 219-236. https://doi.org/10.1007/BF02524225
Tadesse, T., Senay, G. B., Berhan, G., Regassa, T., & Beyen, S. (2015). Evaluating a satellite-based seasonal evapotranspiration product and identifying its relationship with other satellite-derived products and crop yield: A case study for Ethiopia. *International Journal of Applied Earth Observation and Geoinformation, 40*, 39-54. https://doi.org/10.1016/j.jag.2015.03.006
Tolba, R. A., El-Shirbeny, M. A., Abou-Shleel, S. M., & El-Mohandes, M. A. (2020). Rice acreage delineation in the Nile Delta based on thermal signature. *Earth Systems and Environment, 4*, 287-296. https://doi.org/10.1007/s41748-019-00132-x
Valor, E., & Caselles, V. (1996). Mapping land surface emissivity from NDVI: Application to European, African and South American Areas. *Remote Sensing of Environment, 57*(3), 167-184. https://doi.org/10.1016/0034-4257(96)00039-9
Yin, Y., Wu, S., Zheng, D., & Yang, O. (2008). Radiation calibration of FAO56-Penman–Monteith model to estimate reference crop evapotranspiration in China. *Agricultural Water Management, 95*(1), 77-84. https://doi.org/10.1016/j.agwat.2007.09.002
Zhao, S., Yang, Y., Zhang, F., Sui, X., Yao, Y., Zhao, N., Zhao, Q., & Li, C. (2015). Rapid evaluation of reference evapotranspiration in Northern China. *Arabian Journal of Geosciences, 8*, 647-657. https://doi.org/10.1007/s12517-013-1263-0